Ultrasonics Sonochemistry 83 (2022) 105919

Contents lists available at ScienceDirect

Ultrasonics Sonochemistry

journal homepage: www.elsevier.com/locate/ultson

Bacterial cell wall material properties determine *E. coli* resistance to sonolysis

Žiga Pandur [a,b], Matevž Dular [b], Rok Kostanjšek [a], David Stopar [a,*]

[a] University of Ljubljana, Biotechnical Faculty, Večna pot 111, 1000 Ljubljana, SI-Slovenia
[b] University of Ljubljana, Faculty of Mechanical Engineering, Aškerčeva 6, 1000 Ljubljana, SI-Slovenia

ARTICLE INFO

Keywords:
Viability
Bacteria
Escherichia coli
Sonication
Cell envelope

ABSTRACT

The applications of bacterial sonolysis in industrial settings are plagued by the lack of the knowledge of the exact mechanism of action of sonication on bacterial cells, variable effectiveness of cavitation on bacteria, and inconsistent data of its efficiency. In this study we have systematically changed material properties of *E. coli* cells to probe the effect of different cell wall layers on bacterial resistance to ultrasonic irradiation (20 kHz, output power 6,73 W, horn type, 3 mm probe tip diameter, 1 ml sample volume). We have determined the rates of sonolysis decay for bacteria with compromised major capsular polymers, disrupted outer membrane, compromised peptidoglycan layer, spheroplasts, giant spheroplasts, and in bacteria with different cell physiology. The non-growing bacteria were 5-fold more resistant to sonolysis than growing bacteria. The most important bacterial cell wall structure that determined the outcome during sonication was peptidoglycan. If peptidoglycan was remodelled, weakened, or absent the cavitation was very efficient. Cells with removed peptidoglycan had sonolysis resistance equal to lipid vesicles and were extremely sensitive to sonolysis. The results suggest that bacterial physiological state as well as cell wall architecture are major determinants that influence the outcome of bacterial sonolysis.

1. Introduction

Sonication is widely used for dispersing, surface cleaning, degassing, food and beverage processing, medical scanning, nano synthesis, mineral processing, welding, cell disruption, and extraction of cellular components [1–6]. Another promising potential of sonication is disruption and inactivation of bacteria, for example in wastewater treatment plants [7]. The wider application of cavitation for bacterial inactivation is hampered by the lack of the knowledge of the mechanism of action of sonication on bacterial cells, variable effectiveness of cavitation on bacteria, and inconsistent data of its efficiency.

During sonication small vapour bubbles (cavities) form inside an initially homogeneous liquid medium by a sudden decrease in pressure with subsequent cavity collapse [8,9]. From a mechanical point of view the collapse of cavitation bubble produces extreme conditions such as pressure shocks up to several 100 MPa, microjets with velocities above 100 m/s, hot spots with extreme temperatures in order of several 1000 K [10–14]. From a chemical point of view, highly reactive radicals or antimicrobials can be formed due to local high temperatures [15]. In terms of biology, pressure oscillations during bubble collapse modify permeability of cellular membrane (sonoporation), which is useful in cellular transfection or transformation [16] and can be used to inactivate bacteria [17,18].

Concentrated energy during collapse of cavitation bubbles can have major effects on bacterial cell integrity [19]. The exact mechanism of bacteria disruption, however, is not known [1,20–22]. It has been proposed that ultrasound weakens or disrupts bacterial cell envelope structure through a number of processes [1,23].

1. Damage of bacteria cell due to mechanical effects induced by pressure and pressure gradients during the collapse of cavitation bubbles within or near the bacteria.
2. Shear forces induced by microstreaming.
3. Chemical attack due to the formation of free radicals, which attack the cell wall layer structures leading to disintegration.
4. Formation of a bactericidal hydrogen peroxide.

The ability of *Escherichia coli* to survive physico-chemical stress is often related to material properties and multi-layered structure of cell wall [24–28]. *E. coli* cell envelope has cytoplasmic membrane,

* Corresponding author.
E-mail address: david.stopar@bf.uni-lj.si (D. Stopar).

https://doi.org/10.1016/j.ultsonch.2022.105919
Received 21 October 2021; Received in revised form 23 December 2021; Accepted 13 January 2022
Available online 18 January 2022

peptidoglycan layer, outer membrane, capsular layer, slime-layer, loosely attached extracellular polymeric substances, pilli, fimbriae, and flagella [29–32]. Each layer or structure has a unique chemical composition (Fig. 1), which in combination with the other layers form a multi-composite cell envelope structure that resist environmental stresses. The resistance of different cell wall structures to sonication is not known and has not been studied systematically.

Traditionally, peptidoglycan is considered to be the most important pressure bearing element of the bacterial cell envelope [33]. It is composed of glycan strands and peptide stems. The glycan strands are made of alternating N-acetylglucosamine (GlcNAc) and N-acetylmuramic acid (MurNAc) residues linked by β-1–4 glycosidic bonds. To provide mechanical stability glycan strands are cross-linked via peptide stems which generates mesh-like cell wall structure. Its viscoelastic properties allow cell reversible expansion under pressure and together with auxiliary proteins such as MreB give cell its shape [34,35]. Peptidoglycan is one of the most important targets for the action of antibiotics (i.e., ß-lactam antibiotics) and enzymes (i.e., lysozyme). The disruption of peptidoglycan layer causes cell lysis due to osmotic pressure fluctuations [36,37].

The outer membrane is another important structural element that in combination with peptidoglycan resist turgor pressure fluctuations [38,39]. The outer membrane has asymmetrical composition with an inner leaflet rich in phospholipids and an outer leaflet predominantly composed of polyanionic lipopolysaccharides (LPS) [40,41]. The polyanionic nature of LPS with numerous phosphate and acid sugar groups is stabilised by divalent cations (Mg^{2+} and Ca^{2+}). If divalent cations are removed by chelators (i.e., EDTA) the structural integrity of the bacterial outer membrane is severely compromised [42,43].

Additional structural element that strengthens the bacterial cell envelope is capsule [44]. Capsule can extend to great distances from the cell surface (often up to several micrometres) and is used as cementing substance to bind bacteria together or to a surface, and acts as a physical barrier to antibiotics [45–47]. Capsules are composed of high-molecular-weight capsular polysaccharide chains that are linked covalently and noncovalently to the outer membrane [30]. In *E. coli* four major extracellular polymer components have been identified: poly ß-1,6-N-acetyl-D-glucosamine (PGA), curli proteins, colanic acid, and bacterial cellulose or cellulose derivates [48–53]. Recently, their effect on *E. coli* biofilm mechanical properties has been described [54].

In this work we have modified cell wall layers material properties of *E. coli* and probe the resistance of compromised cells to sonolysis. We have determined the rates of sonolysis decay for bacteria with compromised major capsular polymers, disrupted outer membrane, compromised peptidoglycan layer, as well as resistance of spheroplasts and giant spheroplasts (stripped bacterial cells with all cell wall layers removed except cytoplasmic membrane). The integrity of the intact and modified cell envelopes after sonolysis were tested in the exponential and stationary growth phase. The results suggest significantly different contribution of envelope layers to bacterial ability to resist sonolysis.

2. Methods

2.1. Growth and preparation of bacteria with weakened cell wall layers

Two bacterial strains were used in experiments: *E. coli* MG1655 strain with inducible green fluorescent protein (gfp) under IPTG (isopropyl ß-D-1-thiogalactopyranoside) inducible promotor and an isogenic mutant of MG1655 strain (*eps*-) that does not produce ß-1,6-N-acetyl-D-glucosamine (PGA), curli proteins, and colanic acid. Frozen

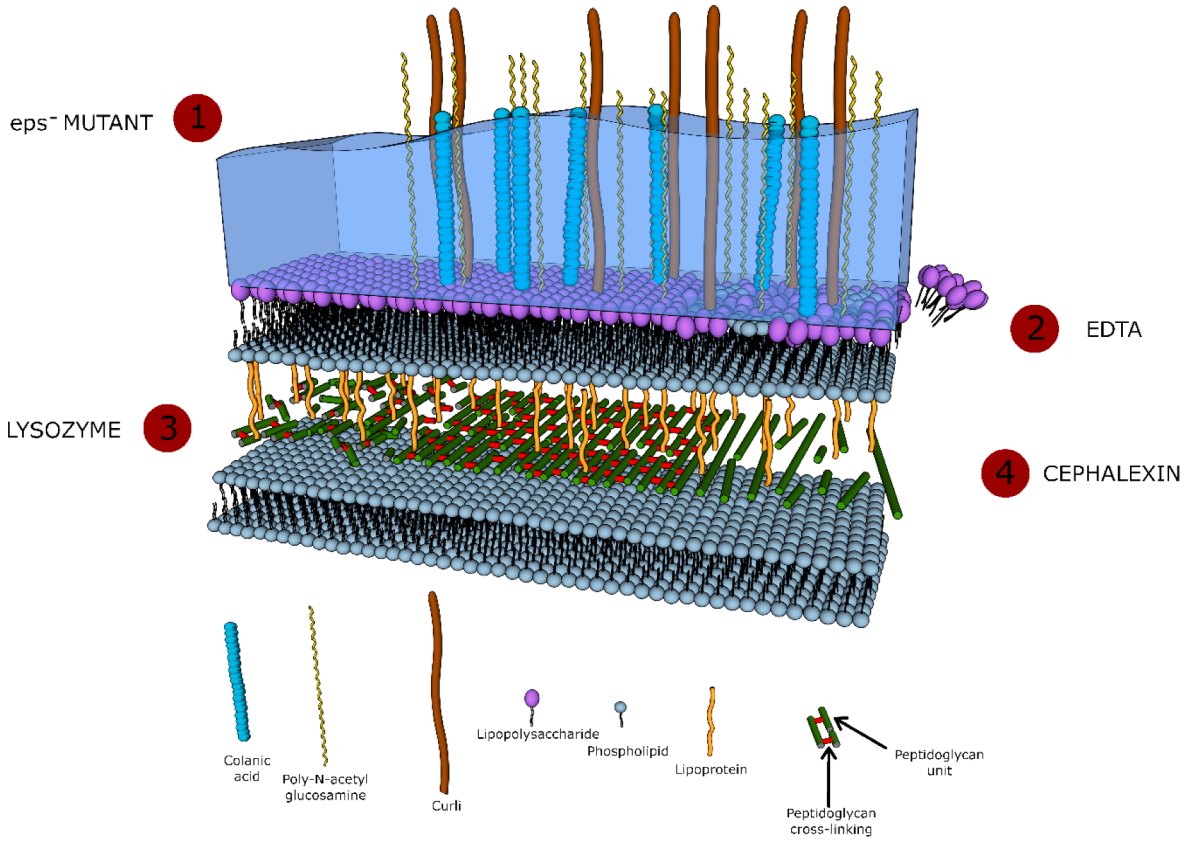

Fig. 1. Cell envelope layer structures that have been modified in different experiments. 1. capsule weakened isogenic *eps*- strain with deletions of genes for synthesis of PGA, colanic acid and curli proteins. 2. Outer membrane weakened by EDTA chelation of divalent ions. 3. Peptidoglycan wakened by lysozyme treatment, which cuts glycan 1–4 β glycosidic bonds. 4. Peptidoglycan weakened with cephalexin that inhibits transpeptidases crosslinking. 5. Combination of treatments (2 + 3) to produce spheroplasts. Combination of treatments (2 + 3 + 4) to produce giant spheroplasts. Depicted are different layers with major chemical constituents.

stock culture from −80 °C were plated on lysogeny broth (LB) agar plates with kanamycin - Kn (50 μg/ml). Bacterial colonies from LB plates were used as inoculum for an overnight culture incubated at 37 °C and shaken at 200 rpm under aerobic conditions. Next, 1 % of overnight medium was inoculated into a fresh LB Kn medium (50 μg/ml kanamycin) and incubated at 37 °C, 200 rpm until the exponential growth phase (optical density OD_{650} of ~ 0,5 a.u) when cells were chemically treated. Experiments were performed also on cells in the stationary growth phase where cells were grown overnight (approx. 18 h incubation time) and then chemically treated.

Several modifications of cell wall layers were performed (Fig. 1). For peptidoglycan modification we used antibiotic cephalexin, which targets penicillin binding protein (PBP3, FtsI) involved in transpeptidases crosslinking [55]. To cells in the exponential or stationary growth phase cephalexin was added to a final concentration of 50 μg/ml. The suspension was incubated for 30 min at the growth conditions. Alternatively, peptidoglycan was modified with lysozyme, which cleaves glycosidic bonds. To the cell culture in the exponential or stationary growth phase we added lysozyme to a final concentration of 100 μg/ml. Cell suspension was incubated for 30 min at the growth conditions.

For the outer membrane modification, we used EDTA to sequester divalent Ca^{2+} and Mg^{2+} ions. The cell culture in the exponential or stationary growth phase was harvested with centrifugation at 4000 RCF for 3 min. Pellet was resuspended in 0,8 M sucrose. To the cell suspension we added EDTA to a final concentration of 3 mM and 25 mM Tris buffer (pH = 8,0). After addition of reagents, cultures were further incubated for 30 min at the growth conditions.

For simultaneous modification of multiple cell wall layers, we produced giant spheroplasts as described by Sun et al. 2014 [56]. Filamentous cells were used to produce giant spheroplasts [57]. Briefly, 4 ml of LB suspension in the exponential growth phase (OD ~ 0,5) was transferred into fresh 36 ml LB medium with cephalexin (50 μg/ml) and kanamycin (50 μg/ml). Bacterial culture was incubated at 37 °C on a shaker at 200 rpm for 2 h. Filamentous cells were harvested with centrifugation at 4000 RCF for 3 min. Pellet was resuspended in 5 ml 0,8 M sucrose to which we have added EDTA to a final concentration of 3 mM, 25 mM Tris buffer (pH = 8,0), and lysozyme to a final concentration of 100 μg/ml. After 10 min of incubation at room temperature, 2 ml of stop solution was added (1 M $MgCl_2$, 0,8 M sucrose, 10 mM Tris-HCl) to inactivate EDTA and to stabilize spheroplasts. For cultivation of filaments with different length, we used protocol described above for the preparation of giant spheroplasts and incubated cells in fresh LB medium with Cephalexin for various total times: 30, 60, 90 and 150 min to obtain filaments up to 90 μm length.

Additionally, we used a combination of EDTA and lysozyme only, which induces formation of smaller sized spherical cell (spheroplast). We followed the same preparation as described above, but without incubation with cephalexin. When removing growth medium, cells in the exponential growth phase were harvested from 40 ml of culture into 5 ml of 0,8 M sucrose, whereas for cells in the stationary growth phase 5 ml of growth medium were harvested into 5 ml 0,8 M sucrose.

2.2. Sonolysis

After preparation of bacterial cultures with modified cell wall envelope structures, 1 ml of samples were aliquoted into microcentrifuge tubes and stored on ice. For sonolysis experiments we used horn probe sonicator (MSE 150 W Ultrasonic disintegrator Mk2) equipped with the exponential probe 168 1/8″ – 3 mm, at nominal frequency of 20 kHz and at 15 μm amplitude. Probe was immersed approximately 15 mm into the liquid volume in a microcentrifuge tube. Samples were sonicated up to 90 s. At sonication times longer than 30 s we have used “duty-cycles”, where 30 s of sonication was followed by 30 s of pause to avoid excessive sample heating, temperature did not exceed 38,1±(0,4) °C.

2.3. Bacterial counts

After sonolysis samples were serially diluted in saline solution (0.9 % NaCl) and plated on LB Kn plates. For samples treated with EDTA or EDTA in combination with lysozyme or cephalexin serial dilutions in 0,8 M sucrose were made to avoid inactivation of EDTA due to the presence of ions in the solution. Culture plates were incubated overnight at 37 °C and next day the number of colony forming units (CFU) were counted. For spheroplasts and giant spheroplasts bacterial counts after sonolysis were made on microscope to avoid counting of viable rod cells that were not transformed during the treatment.

2.4. Microscopy

For visualisation of cell morphology and viability assessment bacterial samples were visualized with fluorescence microscope Zeiss Axio Observer Z1 equipped with laser confocal unit LSM 800. For fluorescence microscopy, the wild-type strain was induced with IPTG (final concentration 40 μM) to induce gfp synthesis, while for the *eps*- mutant we used SYTO-9 fluorescent stain (final concentration 33,4 μM). In both cases we used excitation laser wavelength of 488 nm, and emission filter of 400–585 nm. To observe dead cells, samples were additionally stained with propidium iodide (PI) to a final concentration of 40 μM (excitation laser wavelength: 561 nm, emission filter: 585–700 nm). For accurate microscopic measurement, bacterial sample was fixed with 1 % agarose gel (Thermo Scientific Topvision Low melting point agarose) to prevent excess bacterial motion.

Resistance to sonolysis of spheroplasts and giant spheroplasts was quantified with microscopic image analysis. 10 μL of bacterial sample was put on microscopic glass slide and covered with 20x20 mm #1.5 cover glass. Samples on glass slides were sealed with VALAP sealant (mixture of Vaseline, lanolin and paraffin wax) [58]. Samples were observed under microscope after 5 min of incubation at a room temperature. Microscopic images (4x4 tiled images with 10 % overlay) were acquired through 6 random locations on microscopic glass slide for each treatment time. For spheroplasts we used 100x magnification lens, for giant spheroplasts we used 20x magnification lens. After image acquisition, images were analysed with ImageJ 1.53c software where the spheroplasts were counted.

2.5. Transmission electron microscopy

For transmission electron microscopy (TEM) of bacterial cultures the samples were fixed in 3,5 % glutaraldehyde in 0,1M PBS overnight at 4 °C. After washing the fixative by 0,1 M PBS solution, the bacterial cells were pelleted by 3 min centrifugation at 4000 RCF and resuspended in 3 % low melting-point agarose. Sample was carefully mixed and incubated at room temperature until agarose fully solidified. Agar block was cut into smaller pieces approximately 1x1x1 mm in size, postfixed in 1 % OsO_4 for an hour and rinsed with deionised water. Following dehydration in a series of gradient ethanol concentrations: 50 %, 70 %, 90 %, 96 %, and acetone, samples were embedded in Agar 100 resin (Agar Scientific). Ultrathin sections were transferred to copper grids, contrasted with uranyl acetate and lead citrate and visualized with CM100 (Philips) transmission electron microscope.

2.6. Statistical analysis

Experimental data (either CFU or number of spheroplasts obtained by microscopy) were statistically analysed. The decay rate was obtained by fitting the decrease of bacterial number density during sonolysis with equation Eq. (1).

$$y = y_0 + A_1 e^{-kt} \quad (1)$$

where y_0 represents the initial value, A_1 is amplitude, t is sonication

time, and k is decay rate. Fitted data parameter k of the individual experiments were collected and averaged. The average values were obtained from 5 independent biological experiments. A two-sample *t*-test assuming equal variances were used to test if cell wall layers treatments had significant effect on sonolysis resistance. Additionally, bacterial half-life ($t_{1/2}$) was characterised as described in Eq. (2). Half-life depicts sonication time when half of the viable bacterial population was killed.

$$t_{1/2} = \frac{\ln(2)}{k} \tag{2}$$

2.7. Measurements of sonicator output power

Calorimetric measurement was used to determine the output power of sonicator at 15 μm amplitude. Shortly, 20 ml of water was put in a plastic tube that was thermally isolated with polystyrene. Water was cooled down to 5 °C before starting the experiment. During sonication water temperature was measured every 10 s. The total sonication time was 370 s. The sonicator output power was calculated with Eq. (3),

$$P = \frac{m^{*}c_p{}^{*}\Delta T}{t} \tag{3}$$

where m represents mass of the medium, c_p is heat capacity at constant pressure (for water 4185,5 J/K*kg), ΔT is increase in temperature, and t sonication time. The measured output of sonication power was 6,73±(0,13) W. Furthermore, we have calculated the energy required to reduce bacterial number to half of the initial concentration ($E_{1/2}$) as described in Eq. (4)

$$E_{1/2} = t_{1/2}{}^{*}P \tag{4}$$

where $t_{1/2}$ represents half-life time (Eq. 2) of the viable bacteria during sonication and P is the sonication power.

2.8. ROS detection

For ROS detection during sonication, we performed ROS assay with DTT as a marker. 10 mM solution of DTT was prepared in deionized water. 1 ml of DTT solution was sonicated up to 210 s (in 30 s increments). Generation of ROS was followed with absorbance measurements at 280 nm (oxidized DTT absorbs at 280 nm wavelength). Absorbance was measured on Spectrophotometer (Nanodrop 1000, Thermo Scientific).

3. Results

The effect of low frequency ultrasound sonolysis on a suspension of *E. coli* cells in the exponential and stationary growth phase is shown in Fig. 2. The cell number decayed exponentially. The decay rate was influenced by the physiological state of cells. The exponential cells were significantly more sensitive to sonication than stationary cells. The average decay rate constant (k) was 0,16±(0,02) for the exponential and 0,03±(0,01) for the stationary bacteria. This implies that the stationary cells were on average 5.3-fold more resistant to sonolysis compared to the exponential cells. There was a significant decrease in the number of cells, but no visible cell debris (Supplementary Figure S1). The fraction of the cells with compromised cytoplasmic membrane was low before the ultrasound treatment and increased significantly after the treatment. Although the majority of bacteria lysed, there was a significant fraction of cells that survived sonolysis. The decay rate was not dependent on the initial bacterial densities (results not shown). To determine sonochemical effect we have performed Dithiothreitol (DTT) assay [59]. The results show no significant free radical production during sonication (Supplementary Figure S2).

To probe the effect of different cell wall layers on cell resistance to sonolysis we have modified bacterial cell wall structures and bacterial physiological states. Most of the chemical treatments did not decrease the number of viable cells prior to sonication so in this respect they were not antimicrobial. Only in production of spheroplasts the pre-treatment reduced viability (Supplementary Table S1). The morphologies of modified cells are given in Fig. 3. The exponential cells were rod shaped with dimensions 2,89±(0,67) × 0,74±(0,06) μm, in contrast cells in the stationary growth phase were smaller 1,44±(0,25) × 0,63±(0,06) μm (Fig. 3). When peptidoglycan layer in the exponential cells was modified with antibiotic cephalexin, which inhibits cross-linking of peptidoglycan molecules, cell size increased to 5,84±(0,96) × 0,86±(0,10) μm and cells formed filaments (Fig. 3A). Cephalexin treatment increased volume of the cells by 3.4-fold. On the other hand, cells treated with cephalexin in the stationary growth phase did not enlarge and form filaments. The peptidoglycan layer modified with lysozyme, that catalyses the hydrolysis of 1,4-β-linkages between N-acetylmuramic acid and N-acetyl-D-glucosamine residues in peptidoglycan, had little effect on bacterial morphology and membrane integrity both in the exponential and stationary growth phase. Cells in the exponential growth phase treated with EDTA had the same size but severely compromised membranes as indicated by increased permeability to PI dye. Contrary, cells in the

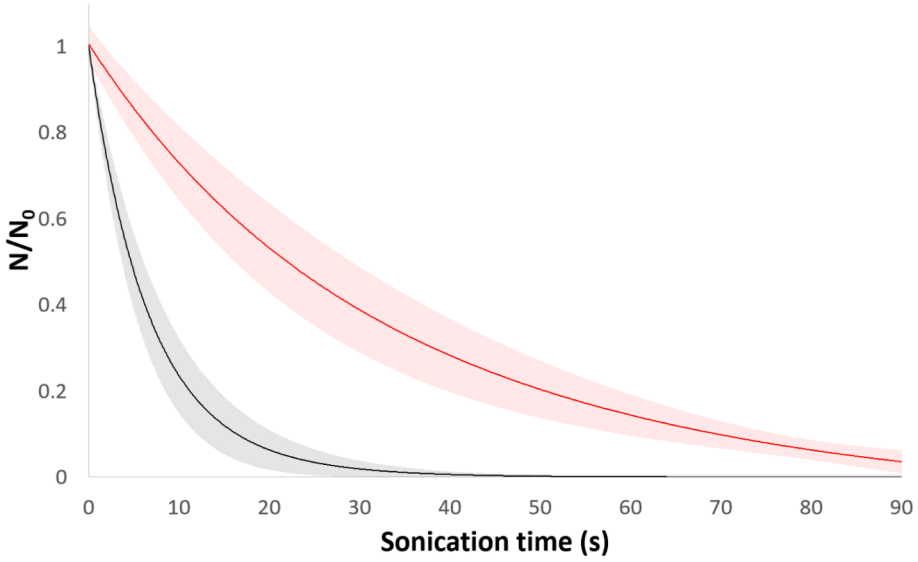

Fig. 2. Decay curves of exponential (black line) and stationary (red line) *E. coli* cells during sonication. Data were normalized to the initial bacterial numbers and fitted with Eq. 1. The mean decay curves with colour shaded bands representing standard deviations are shown (n = 5).

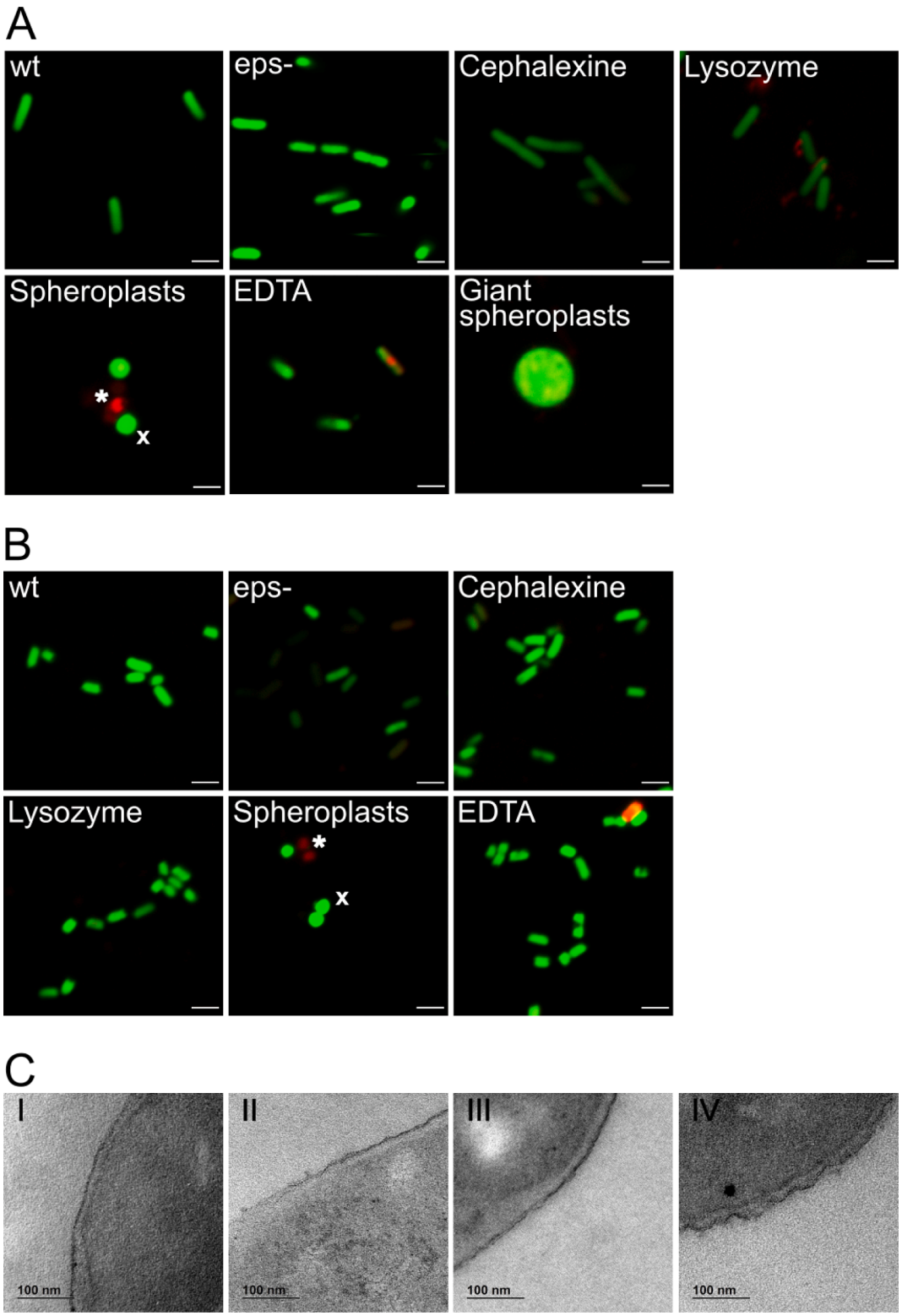

Fig. 3. Morphology of *E. coli* after different treatments that affect cell wall layer structure in the exponential (A) and stationary growth phase (B). Microscopic images are composite images from gfp (green fluorescence protein – indicating viable bacteria) and PI (red propidium iodide – indicating bacteria with compromised membrane). In spheroplast images, viable cells are indicated with "x" and cells with compromised membranes with "*". Scale bar represents 5 μm. (C) TEM micrographs of *E. coli* cells: (I) untreated cells in the exponential growth phase, (II) untreated cells in the stationary growth phase, (III) *eps*- mutant in stationary growth phase, and (IV) cephalexin treated cells in exponential growth phase.

stationary growth phase were much less sensitive to EDTA treatment. The combined EDTA and lysozyme treatment resulted in spheroplast formation. Spheroplast formation reduced the number of viable cells (Supplementary Table S1). The cells that remained viable had spherical morphology with an average diameter of 2,3±(0,4) μm. When cells were treated with a combination of EDTA, lysozyme, and cephalexin giant spheroplast formed, with a diameter of 4,5±(1,0) μm. Giant spheroplasts could not be produced in the stationary growth phase because cephalexin does not work on non-growing cells. In general, in the stationary growth phase, most of the treatments did not have a significant impact on morphology. The exception was a combination of EDTA and lysozyme, which produced spheroplasts. TEM micrographs reveal similar cell wall ultrastructure for the exponential and stationary cells (Supplementary Figure S4). The cephalexin treated cells had higher degree of wrinkling of the cell wall observed with TEM (Fig. 3 and Supplementary Figure S5). There was no visible difference in cell wall ultrastructure for the *eps-* mutant.

Cells with modified cell wall layers had different sensitivity for sonolysis (Fig. 4). For example, cells treated with cephalexin in the exponential growth phase showed significantly larger decay rate 0,53± (0,8) compared to cephalexin untreated cells 0,16±(0,02). In cephalexin treated cells already after 10 s of sonication the fraction of viable cells was lower than 0.01. In contrast, cells in the stationary growth phase were insensitive to cephalexin treatment and there was no significant difference in sonolysis decay rate compared to untreated cells.

The effects of other cell wall layer modifications on sonolysis decay rates are given in Fig. 5A. Different treatments had no effect on stationary bacteria, except for spheroplasts, which were significantly more sensitive than untreated stationary cells. On the other hand, the exponential cells were much more sensitive to sonication (larger k values) and respond differently to cell wall modifications. Treatment with cephalexin, formation of spheroplasts, and formation of giant spheroplasts had a large effect on bacterial sensitivity to sonolysis. In particular, the giant spheroplast were very sensitive to sonolysis. Contrary, the removal of capsular polymers (*eps-* mutant), the outer membrane (EDTA), and lysozyme treatment did not change bacterial sensitivity to sonolysis.

The energy input to reduce viable bacteria to a half of their initial density was significantly lower for the growing compared to non-growing bacteria 29,6±(4,3) and 170±(70) J, respectively (Fig. 5B). For growing bacteria similar energy input was needed to reduce the bacterial number for lysozyme or EDTA treated cells as well as *eps-* mutant strain. The least energy was required for cephalexin treated cells and giant spheroplast 8,9±(1,3) J and 7,1±(3,0) J, respectively.

The effect of bacterial size on decay rate is given in Fig. 6. The results suggest three qualitatively different decay rate regimes. The smallest stationary cells had the lowest decay rate. Slightly larger exponential cells had significantly higher decay rate (on average 8.5-fold). Exponential cells with modified peptidoglycan layer (giant spheroplast, filaments) had the largest decay rate (on average 3.8-fold larger compared to the unmodified cells in the exponential phase). Increasing the length of the filament by Cephalexin treatment (from 5 to 90 μm), had only a limited effect on decay rate (1.45-fold increase).

4. Discussion

There are numerous proposed mechanisms of sonication that affect viability of bacteria [1,23] (i.e. physical, chemical, mechanical, biological) that occur simultaneously during sonication treatment. In this work we have focused on different cell wall layers material properties and their contributions to bacterial resistance to cavitation and sonolysis. This has not been described yet in the literature and provides a foundation for a successful application of sonolysis. As sonochemical effects do not contribute significantly (Supplementary Figure S2) to bacterial decay rate, in accordance with literature on low frequency sonication [60–62], we will mainly discuss bacterial mechanical properties and their effect on sonolysis resistance. The data suggest that cell size can have an effect on decay rate (Fig. 6). However, as cell wall architecture and cell physiological status have significantly larger effect on cell decay rates they will be primarily discussed.

The outermost cell layer modified was the capsular layer (*eps-* mutant in Fig. 1). The results suggest that removing the capsular polymers such as PGA, colanic acid, and curli proteins did not significantly increase sensitivity to sonication. Capsular components are synthesised more extensively under stress conditions (i.e., stationary growth phase) [63–65]. However, neither the exponential nor the stationary bacteria with removed capsular polymers (*eps-* mutant) were more sensitive to sonolysis than the wild type. This suggests that these components do not provide protection against sonolysis. In our previous work we have shown that capsular polymers determine rheological behaviour of *E. coli* biofilms [54]. In particular, they contribute to biofilm cohesive energy and are important in establishing intercellular bacterial stress resistant

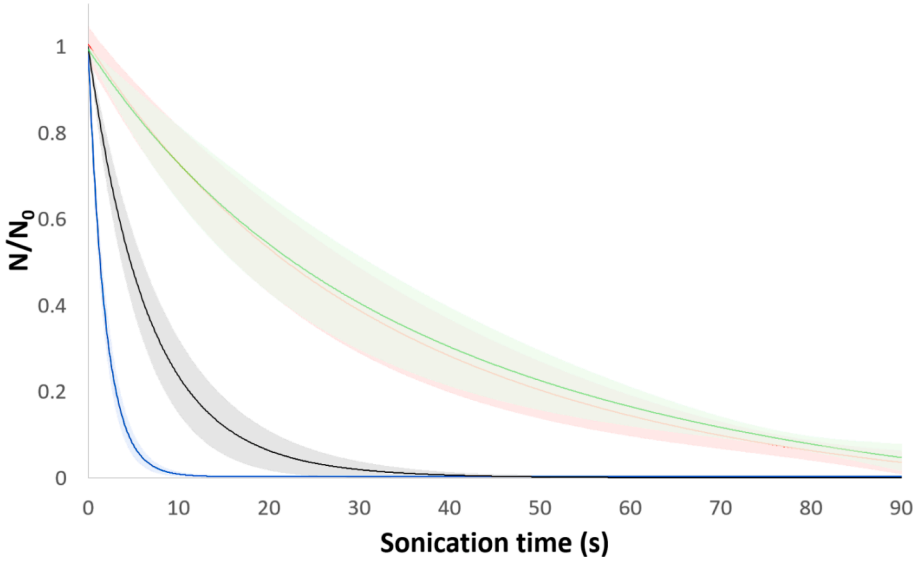

Fig. 4. Decay curves of cephalexin untreated (black line) and cephalexin treated (blue line) exponential cells, and cephalexin untreated (red line) and cephalexin treated (green line) stationary cells. The data were fitted with Eq. 1. The mean decay curves with colour shaded bands representing standard deviations are shown (n = 5).

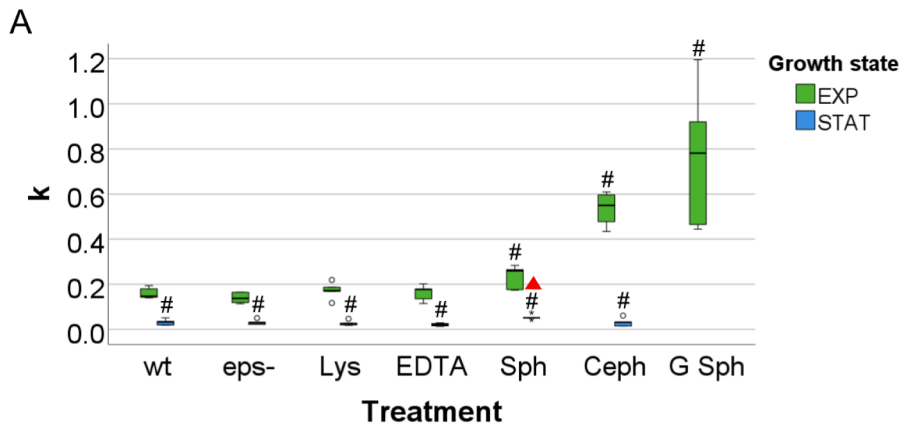

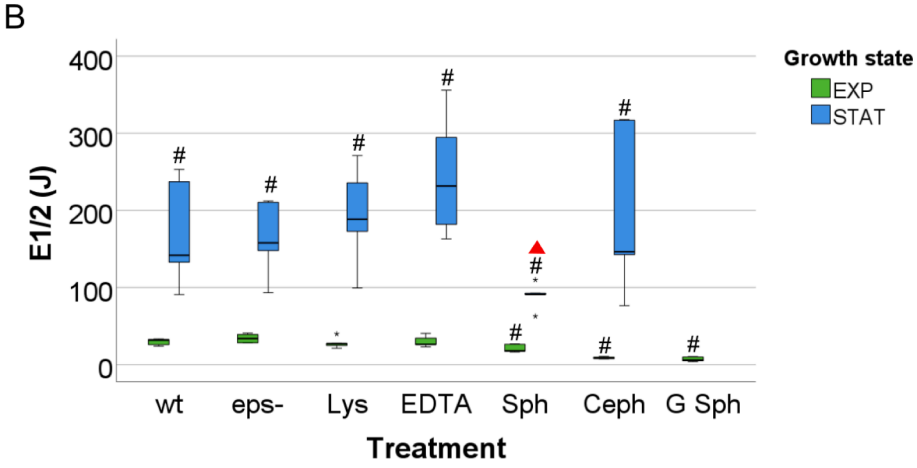

Fig. 5. (**A**) Sonication decay rate *k* and (**B**) cumulative energy required to halve the population of cells for the wild-type *E. coli* strain (wt) and cells with modified cell wall material properties for the exponential (green bars) and stationary cells (blue bars). The box plots are given (n = 5). Black hashtag (#) indicate significant (α = 0,05) difference in decay rates compared to the wild-type strain in the exponential growth phase. Red triangle (▲) shows significant (α = 0,05) difference to the wild-type strain in the stationary growth phase. Abbreviations: wt (untreated cells), eps- (cells with removed capsular polymers), Lys (cells treated with lysozyme), EDTA (cells treated with EDTA), Sph (spheroplasts, cells treated with lysozyme and EDTA), Ceph (cells treated with Cephalexin), G Sph (giant spheroplasts, cells treated with Cephalexin, lysozyme and EDTA).

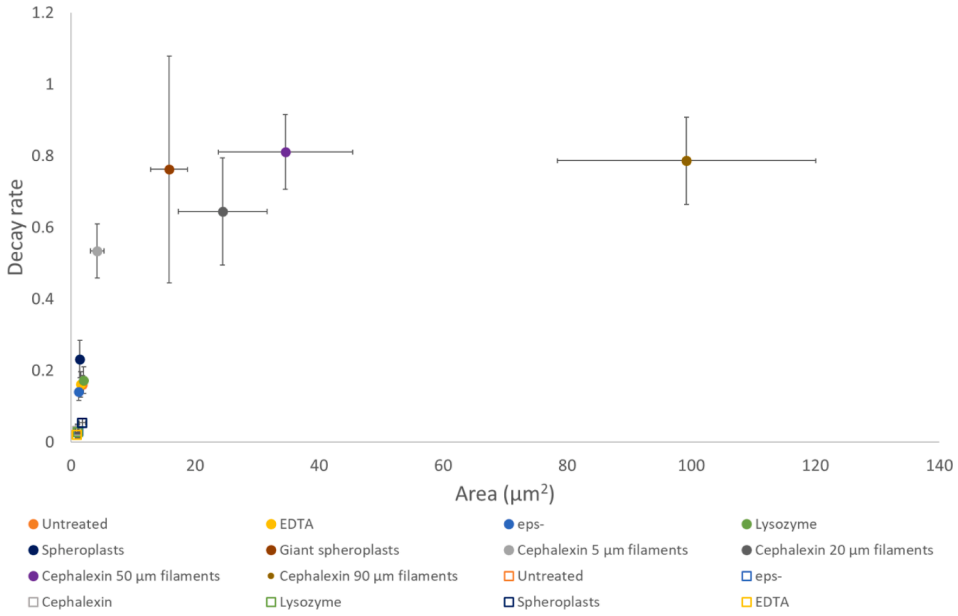

Fig. 6. The effect of cell size (presented as area of the cell) on sonication decay rate. Dots represent cells in the exponential growth phase, hollow squares represent cells in the stationary growth phase.

structures. We conclude that capsular layer does not contribute significantly to *E. coli* ultrasound resistance.

Cells treated with EDTA (Fig. 1), which weakens the outer membrane, had higher envelope permeability to PI dye in the exponential growth phase (Fig. 3A), but were not more sensitive to sonolysis. Chelation of divalent cations with EDTA extracts divalent metal ions such as Ca^{2+} and Mg^{2+} from their binding sites within the outer membrane, weakening the LPS interactions [43]. In the presence of EDTA, the outer membrane loses its structural integrity and vast quantities (up to 50 % of total LPS) are released into solution [66–69]. The loss of LPS

molecules corresponds to appearance of irregularly shaped pits, bumps and dents along with rougher cell surface [42,70] that reduces envelope and cell stiffness [39]. Recently researchers observed increased permeability of the outer and inner membrane during sonication [71,72]. Additionally, sonication increased membrane rigidity and decreased membrane potential [71]. Although we have observed increased envelope permeability in EDTA treated cells we did not observe significant difference in sonolysis resistance, which suggest that the outer membrane structure does not contribute significantly to *E. coli* ultrasound resistance.

Peptidoglycan maintains bacterial shape and protects cytoplasmic membrane from turgor pressure stress [73]. We have used two external peptidoglycan modifications: treatment with antibiotic cephalexin and with enzyme Lysozyme. Cephalexin is an antibiotic that irreversibly binds to and inactivates penicillin-binding proteins (PBPs) which interferes with cross-linking of peptide chains necessary for peptidoglycan strength and rigidity (Fig. 1) [36,74]. Cells treated with cephalexin were significantly more sensitive to sonolysis. Cephalexin is also used as a septation inhibitor for production of *E. coli* filaments [56,75,76]. Consistent with the literature we have observed filament morphology in the exponential cells treated with cephalexin (Fig. 3A and S3). It is interesting to note that filament cells were significantly more sensitive to sonolysis compared to the individual rod-shaped bacteria. Increasing the size of filaments for approximately 20 fold resulted in 1.4 increase in sonolysis sensitivity, which suggest that bacterial size has a small effect. In the stationary growth phase cephalexin did not induce morphological changes and did not sensitise cells for sonolysis. These results imply that actively grown cells with weakened peptidoglycan layer, but otherwise intact outer membrane and capsular layer, are sensitive to sonolysis.

Peptidoglycan can be weakened also by enzymatic hydrolysis of glycoside bonds with lysozyme (1,4-β-N-acetylmuramidase), which leads to cell envelope instability (Fig. 1) [37]. The addition of lysozyme did not sensitise cells for sonolysis. In Gram-negative organisms such as *E. coli* the action of lysozyme may be hindered because the outer membrane shields peptidoglycan from the external environment [77]. Due to the absence of morphology changes, changes of permeability, or sonolysis decay rate we infer that lysozyme did not reach peptidoglycan (Fig. 3) [42]. To increase the access of lysozyme to its target we have combined lysozyme treatment with EDTA. After a combined treatment cells changed shape and become spherical, a clear indication of peptidoglycan modification (Fig. 3). It is generally accepted that spheroplasts have partially removed outer membrane and peptidoglycan layer but keep the intact cytoplasmic membrane [43,57,78,79]. The results indicate that spheroplasts are very sensitive to sonolysis (Table S1) both in the exponential and stationary growth phase.

The combination of lysozyme, EDTA, and cephalexin produced giant spheroplasts (Fig. 3.) that were extremely sensitive to sonolysis (Fig. 5A). In a combined action EDTA permeabilizes the outer membrane, which in turn permits lysozyme to cross into the periplasmic space, where together with cephalexin completely degrades peptidoglycan thus allowing the formation of giant spheroplasts [42,80]. We observed that giant spheroplasts had increased permeability for PI dye and lower viability. When giant spheroplasts were sonicated, they rapidly lose viability. Essentially, a giant spheroplast represents a giant lipid bilayer vesicle. Previously we have shown that giant DOPC lipid vesicles are very sensitive to hydrodynamic and ultrasound cavitation [81]. When compared to other chemical, physical and mechanical stressors such as ionic strength and osmolarity agents, free radicals, shear stresses, high pressure, electroporation, centrifugation, surface active agents, microwave irradiation, heating, and freezing-thawing, ultrasound and hydrodynamic cavitation were among the most powerful. The giant DOPC vesicles were destroyed in less than 5 s at 20 kHz and amplitude of 10 μm [81]. The results of decay of spheroplasts are consistent with lipid vesicle studies [82] and suggest that unprotected cytoplasmic membrane found in spheroplasts can be easily destroyed by cavitation. This also explains why animal cells, which do not have extra protective layers to stabilise cytoplasmic membrane, are very sensitive to sonication [83].

The results of Cephalexin, EDTA, and lysozyme support the main conclusion that peptidoglycan contribute significantly to *E. coli* ultrasound resistance. Peptidoglycan is a complex molecule in which material properties, composition, architecture, and biophysical properties vary with bacterial strain, physiological conditions, and growth phase [84]. It is viscoelastic solid that allows reversible expansion under pressure and gives cell its shape. Normally peptidoglycan is under dynamic stress in the living cell due to the cell turgor pressure. In rod shaped bacteria it is more deformable in the direction of the long axis of the cell (elastic modulus $2.5 \times 10^7 \mathrm{N\ m^{-2}}$) than in the direction perpendicular to the long axis (elastic modulus, $4.5 \times 10^7 \mathrm{N\ m^{-2}}$) [85]. This is consistent with the observation that changes in the volume of osmotically shocked *E. coli* cells are mainly due to changes in the cell length, whereas cell diameter is virtually constant [86]. It was suggested that the anisotropy in elasticity of rod-shaped bacteria is the consequence of the predominant alignment of the flexible peptides in the direction of the long axis of the cell and of the more rigid glycan strands perpendicular to the direction of the long axis [87]. Cephalexin, which prevents peptide cross-linking in the direction of the long axis, had the largest effect on sonolysis decay rate. This suggest that the weakest point during sonication is the cell long axis, where cytoplasmic membrane during sonoporation likely becomes leaky. It was shown that spherical bacteria are more resistant to sonication treatments than rod shaped bacteria [23]. It should be noticed that in spherical bacteria cell peptidoglycan is fully developed and mechanical stress is isotropically distributed with no weak links as in rod shaped bacteria. Spheroplasts on the other hand have spherical geometry, but they do not possess functional peptidoglycan layer, which makes them extremely vulnerable to sonolysis.

In all experiments we have observed that stationary cells were significantly more resistant to sonolysis than exponential cells. This is likely the consequence of peptidoglycan remodelling. It has been shown that during the transition of *E. coli* from an exponential to a stationary phase the material properties, composition, and architecture of peptidoglycan are dramatically modified. For example, the relative abundance of ld-A2pm-A2pm cross-linked muropeptides increases from approximately 5 to 12 % of the total muropeptides [88], the degree of cross-linkage increases from 28 to 38 % cross-linked muropeptides, the mean glycan chain length decreases from roughly 33 down to 17 disaccharides per chain, and the lipoprotein-bound muropeptides increases from 9 to 14 % [88–90]. Such a remodelling of peptidoglycan increases the resistance to sonolysis. This has an important consequence for the application of sonolysis (i.e. water distribution systems). In these environments there are relatively few nutrients available for bacterial growth and bacteria are mostly starving [91]. Technically such bacteria are in the stationary growth phase and are significantly more resistant to sonolysis than actively growing cells.

5. Conclusions

In conclusion, variable effectiveness of cavitation on bacteria that have been reported in the literature provide an obstacle for implementation of cavitation in industrial settings. The results of this study imply that the most important bacterial structure that determines the outcome during sonication (20 kHz, output power 6,73 W, horn type, 3 mm probe tip diameter, 1 ml sample volume) is peptidoglycan. If peptidoglycan is remodelled, weakened, or absent the cavitation can be very efficient. Weakened peptidoglycan can be found in actively growing bacterial cells or cells that have been chemically treated with antibiotics or enzymes. In cells that lack peptidoglycan such as spheroplasts or eukaryotic cells sonoporation of cell membranes is much more effective and quickly kills cells.

Declaration of Competing Interest

The authors declare that they have no known competing financial interests or personal relationships that could have appeared to influence the work reported in this paper.

Acknowledgments

The authors acknowledge the financial support from the European Research Council (ERC) under the European Union's Framework Program for research and innovation, H2020-EU.1.1. (Grant agreement ID: 771567) and the Slovenian Research Agency (Core funding No. P2-0401 and P4-0116). We acknowledge the financial support from the Slovenian Research Agency to the Infrastructural Centre "Microscopy of Biological Samples", at Biotechnical faculty, University of Ljubljana, member of MRIC UL network.

Appendix A. Supplementary data

Supplementary data to this article can be found online at https://doi.org/10.1016/j.ultsonch.2022.105919.

References

[1] M. Zupanc, Ž. Pandur, T. Stepišnik Perdih, D. Stopar, M. Petkovšek, M. Dular, Effects of cavitation on different microorganisms: The current understanding of the mechanisms taking place behind the phenomenon. A review and proposals for further research, Ultrason. Sonochem. 57 (2019) 147–165, https://doi.org/10.1016/j.ultsonch.2019.05.009.
[2] A.S. Peshkovsky, S.L. Peshkovsky, S. Bystryak, Scalable high-power ultrasonic technology for the production of translucent nanoemulsions, Chem. Eng. Process. Process Intensif. 69 (2013) 77–82, https://doi.org/10.1016/j.cep.2013.02.010.
[3] J.P. Canselier, H. Delmas, A.M. Wilhelm, B. Abismaïl, Ultrasound emulsification - An overview, J. Dispers. Sci. Technol. 23 (1-3) (2002) 333–349, https://doi.org/10.1080/01932690208984209.
[4] D.G. Eskin, K. Al-Helal, I. Tzanakis, Application of a plate sonotrode to ultrasonic degassing of aluminum melt: Acoustic measurements and feasibility study, J. Mater. Process. Technol. 222 (2015) 148–154, https://doi.org/10.1016/j.jmatprotec.2015.03.006.
[5] H.V. Annegowda, R. Bhat, L. Min-Tze, A.A. Karim, S.M. Mansor, Influence of sonication treatments and extraction solvents on the phenolics and antioxidants in star fruits, J. Food Sci. Technol. 49 (4) (2012) 510–514, https://doi.org/10.1007/s13197-011-0435-8.
[6] N. Saranya, P. Devi, S. Nithiyanantham, R. Jeyalaxmi, Cells Disruption by Ultrasonication, Bionanoscience. 4 (4) (2014) 335–337, https://doi.org/10.1007/s12668-014-0149-2.
[7] P. Foladori, B. Laura, A. Gianni, Z. Giuliano, Effects of sonication on bacteria viability in wastewater treatment plants evaluated by flow cytometry-Fecal indicators, wastewater and activated sludge, Water Res. 41 (1) (2007) 235–243, https://doi.org/10.1016/j.watres.2006.08.021.
[8] J.-P. Franc, J.-M. Michel, Fundamentals of Cavitation, Kluwer Academic Publishers, Dordrecht (2005), https://doi.org/10.1007/1-4020-2233-6.
[9] T.J. Mason, Ultrasonic cleaning: An historical perspective, Ultrason. Sonochem. 29 (2016) 519–523, https://doi.org/10.1016/j.ultsonch.2015.05.004.
[10] C.E. Brennen, Cavitation and bubble dynamics, Oxford University Press, Oxford, 1995.
[11] G.L. Chahine, C.-T. Hsiao, Modelling cavitation erosion using fluid–material interaction simulations, Interface Focus. 5 (5) (2015) 20150016, https://doi.org/10.1098/rsfs.2015.0016.
[12] K.S. Suslick, N.C. Eddingsaas, D.J. Flannigan, S.D. Hopkins, H. Xu, Extreme conditions during multibubble cavitation: Sonoluminescence as a spectroscopic probe, Ultrason. Sonochem. 18 (4) (2011) 842–846, https://doi.org/10.1016/j.ultsonch.2010.12.012.
[13] M. Petkovšek, M. Hočevar, M. Dular, Visualization and measurements of shock waves in cavitating flow, Exp. Therm. Fluid Sci. 119 (2020) 110215, https://doi.org/10.1016/j.expthermflusci.2020.110215.
[14] M. Dular, T. Požar, J. Zevnik, R. Petkovšek, High speed observation of damage created by a collapse of a single cavitation bubble, Wear. 418–419 (2019) 13–23, https://doi.org/10.1016/j.wear.2018.11.004.
[15] S. Koda, T. Kimura, T. Kondo, H. Mitome, A standard method to calibrate sonochemical efficiency of an individual reaction system, Ultrason. Sonochem. 10 (3) (2003) 149–156, https://doi.org/10.1016/S1350-4177(03)00084-1.
[16] Y. Song, T. Hahn, I.P. Thompson, T.J. Mason, G.M. Preston, G. Li, L. Paniwnyk, W. E. Huang, Ultrasound-mediated DNA transfer for bacteria, Nucleic Acids Res. 35 (2007) 1–9, https://doi.org/10.1093/nar/gkm710.
[17] A. Šarc, J. Kosel, D. Stopar, M. Oder, M. Dular, Removal of bacteria Legionella pneumophila, Escherichia coli, and Bacillus subtilis by (super)cavitation, Ultrason. Sonochem. 42 (2018) 228–236, https://doi.org/10.1016/j.ultsonch.2017.11.004.
[18] A. Šarc, M. Oder, M. Dular, Can rapid pressure decrease induced by supercavitation efficiently eradicate Legionella pneumophila bacteria? Desalin. Water Treat. 57 (5) (2016) 2184–2194, https://doi.org/10.1080/19443994.2014.979240.
[19] P. Piyasena, E. Mohareb, R.C. McKellar, Inactivation of microbes using ultrasound: A review, Int. J. Food Microbiol. 87 (3) (2003) 207–216, https://doi.org/10.1016/S0168-1605(03)00075-8.
[20] C.W. Ho, T.K. Chew, T.C. Ling, S. Kamaruddin, W.S. Tan, B.T. Tey, Efficient mechanical cell disruption of Escherichia coli by an ultrasonicator and recovery of intracellular hepatitis B core antigen, Process Biochem. 41 (8) (2006) 1829–1834, https://doi.org/10.1016/j.procbio.2006.03.043.
[21] M. Cameron, L.D. McMaster, T.J. Britz, Electron microscopic analysis of dairy microbes inactivated by ultrasound, Ultrason. Sonochem. 15 (6) (2008) 960–964, https://doi.org/10.1016/j.ultsonch.2008.02.012.
[22] L.i. Zhang, Y. Jin, Y. Xie, X. Wu, T. Wu, Releasing polysaccharide and protein from yeast cells by ultrasound: Selectivity and effects of processing parameters, Ultrason. Sonochem. 21 (2) (2014) 576–581, https://doi.org/10.1016/j.ultsonch.2013.10.016.
[23] E. Joyce, A. Al-Hashimi, T.J. Mason, Assessing the effect of different ultrasonic frequencies on bacterial viability using flow cytometry, J. Appl. Microbiol. 110 (2011) 862–870, https://doi.org/10.1111/j.1365-2672.2011.04923.x.
[24] D. Scott Cayley, H.J. Guttman, M. Thomas Record, Biophysical characterization of changes in amounts and activity of Escherichia coli cell and compartment water and turgor pressure in response to osmotic stress, Biophys. J. 78 (4) (2000) 1748–1764.
[25] M. Reuter, N.J. Hayward, S.S. Black, S. Miller, D.T.F. Dryden, I.R. Booth, Mechanosensitive channels and bacterial cell wall integrity: Does life end with a bang or a whimper? J. R. Soc. Interface. 11 (91) (2014) 20130850, https://doi.org/10.1098/rsif.2013.0850.
[26] J. Lee, Gonul Kaletunc, Evaluation of the heat inactivation of Escherichia coli and Lactobacillus plantarum by differential scanning calorimetry, Appl. Environ. Microbiol. 68 (11) (2002) 5379–5386, https://doi.org/10.1128/AEM.68.11.5379-5386.2002.
[27] P. Small, D. Blankenhorn, D. Welty, E. Zinser, J.L. Slonczewski, Acid and base resistance in Escherichia coli and Shigella flexneri: Role of rpoS and growth pH, J. Bacteriol. 176 (6) (1994) 1729–1737, https://doi.org/10.1128/jb.176.6.1729-1737.1994.
[28] K.J.A. Hauben, K. Bernaerts, C.W. Michiels, Protective effect of calcium on inactivation of Escherichia coli by high hydrostatic pressure, J. Appl. Microbiol. 85 (4) (1998) 678–684, https://doi.org/10.1111/j.1365-2672.1998.00577.x.
[29] U.B. Sleytr, B. Schuster, E.-M. Egelseer, D. Pum, S-layers: principles and applications, FEMS Microbiol. Rev. 38 (5) (2014) 823–864, https://doi.org/10.1111/1574-6976.12063.
[30] T.J. Beveridge, L.L. Graham, Surface layers of bacteria, Microbiol. Rev. 55 (1991) 684–705. http://www.ncbi.nlm.nih.gov/pubmed/1723487.
[31] C. Whitfield, Bacterial extracellular polysaccharides, Can. J. Microbiol. 34 (4) (1988) 415–420, https://doi.org/10.1139/m88-073.
[32] A.B. Jonson, S. Normark, M. Rhen, Fimbriae, pili, flagella and bacterial virulence, Contrib. Microbiol. 12 (2005) 67–89, https://doi.org/10.1159/000081690.
[33] A. Typas, M. Banzhaf, C.A. Gross, W. Vollmer, From the regulation of peptidoglycan synthesis to bacterial growth and morphology, Nat. Rev. Microbiol. 10 (2) (2012) 123–136, https://doi.org/10.1038/nrmicro2677.
[34] W. Margolin, Sculpting the Bacterial Cell, Curr. Biol. 19 (17) (2009) R812–R822, https://doi.org/10.1016/j.cub.2009.06.033.
[35] H. Jiang, F. Si, W. Margolin, S. Sun, Mechanical Control of Bacterial Cell Shape, Biophys. J. 101 (2) (2011) 327–335, https://doi.org/10.1016/j.bpj.2011.06.005.
[36] C.J. Harrison, D. Bratcher, Cephalosporins, Cephalosporins : A Review 29 (8) (2008) 264–273.
[37] R.T. Ellison, T.J. Giehl, Killing of gram-negative bacteria by lactoferrin and lysozyme, J. Clin. Invest. 88 (4) (1991) 1080–1091, https://doi.org/10.1172/JCI115407.
[38] J.W. Shaevitz, Microbiology: Peeling Back the Layers of Bacterial Envelope Mechanics, Curr. Biol. 28 (20) (2018) R1210–R1211, https://doi.org/10.1016/j.cub.2018.09.023.
[39] E.R. Rojas, G. Billings, P.D. Odermatt, G.K. Auer, L. Zhu, A. Miguel, F. Chang, element in Gram-negative bacteria, (2018).
[40] A.V. Hughes, D.S. Patel, G. Widmalm, J.B. Klauda, L.A. Clifton, W. Im, Physical Properties of Bacterial Outer Membrane Models: Neutron Reflectometry & Molecular Simulation, Biophys. J. 116 (6) (2019) 1095–1104, https://doi.org/10.1016/j.bpj.2019.02.001.
[41] B. Bertani, N. Ruiz, J.M. Slauch, Function and Biogenesis of Lipopolysaccharides, EcoSal Plus. 8 (1) (2018), https://doi.org/10.1128/ecosalplus.ESP-0001-2018.
[42] N.A. Amro, L.P. Kotra, K. Wadu-Mesthrige, A. Bulychev, S. Mobashery, G.Y. Liu, High-resolution atomic force microscopy studies of the Escherichia coli outer membrane: structural basis for permeability, Langmuir. 16 (2000) 2789–2796, https://doi.org/10.1021/la991013x.
[43] L.A. Clifton, M.W.A. Skoda, A.P. Le Brun, F. Ciesielski, I. Kuzmenko, S.A. Holt, J. H. Lakey, Effect of Divalent Cation Removal on the Structure of Gram-Negative Bacterial Outer Membrane Models, Langmuir. 31 (1) (2015) 404–412, https://doi.org/10.1021/la504407v.
[44] G.R.d.S. Araújo, N.B. Viana, F. Gómez, B. Pontes, S. Frases, The mechanical properties of microbial surfaces and biofilms, Cell Surf. 5 (2019) 100028, https://doi.org/10.1016/j.tcsw.2019.100028.
[45] J.W. Costerton, R.T. Irvin, K.J. Cheng, The bacterial glycocalyx in nature and disease, Annu. Rev. Microbiol. 35 (1) (1981) 299–324.

[46] M.E. Bayer, H. Thurow, Polysaccharide capsule of Escherichia coli: microscope study of its size, structure, and sites of synthesis, J. Bacteriol. 130 (1977) 911–936. http://www.ncbi.nlm.nih.gov/pubmed/400798.
[47] I.S. Roberts, The Biochemistry and genetics of capsular polysaccharide production in bacteria, Annu. Rev. Microbiol. 50 (1) (1996) 285–315, https://doi.org/10.1146/annurev.micro.50.1.285.
[48] X. Wang, X. Wang, J.F.P. Iii, J.F.P. Iii, T. Romeo, T. Romeo, The pgaABCD Locus of Escherichia coli Promotes the Synthesis of a Polysaccharide Adhesin Required for Biofilm Formation, J. Bacteriol. 186 (2004) 2724–2734, https://doi.org/10.1128/JB.186.9.2724.
[49] Y. Itoh, X. Wang, B.J. Hinnebusch, J.F.P. Iii, Depolymerization of ß-1,6-N-Acetyl-D-Glucosamine Disrupts the Integrity of Diverse Bacterial Biofilm, J. Bac. 187 (2005) 382–387, https://doi.org/10.1128/JB.187.1.382.
[50] Y. Itoh, J.D. Rice, C. Goller, A. Pannuri, J. Taylor, J. Meisner, T.J. Beveridge, J. F. Preston, T. Romeo, Roles of pgaABCD genes in synthesis, modification, and export of the Escherichia coli biofilm adhesin poly-β-1,6-N-acetyl-D-glucosamine, J. Bacteriol. 190 (2008) 3670–3680, https://doi.org/10.1128/JB.01920-07.
[51] D. Smith, J. Price, P. Burby, L. Blanco, J. Chamberlain, M. Chapman, The production of curli amyloid fibers is deeply integrated into the biology of escherichia coli, Biomolecules. 7 (4) (2017) 75, https://doi.org/10.3390/biom7040075.
[52] P.N. Danese, L.A. Pratt, Exopolysaccharide Production Is Required for Development of, Society. 182 (2000) 3593–3596, https://doi.org/10.1093/aje/kwi220.
[53] W. Thongsomboon, D.O. Serra, A. Possling, C. Hadjineophytou, R. Hengge, L. Cegelski, Phosphoethanolamine cellulose: A naturally produced chemically modified cellulose, Science (80-.) 359 (2018) 334–338.
[54] M. Horvat, A. Pannuri, T. Romeo, I. Dogsa, D. Stopar, Viscoelastic response of Escherichia coli biofilms to genetically altered expression of extracellular matrix components, Soft Matter. 15 (25) (2019) 5042–5051.
[55] H.S. Chung, Z. Yao, N.W. Goehring, R. Kishony, J.B. Kahne, Rapid β-lactam-induced lysis requires successful assembly of the cell division machinery, Proc. Natl. Acad. Sci. U. S. A. 106 (2009) 21872–21877, https://doi.org/10.1073/pnas.0911674106.
[56] Y. Sun, T.-L. Sun, H. Huang, Physical Properties of Escherichia coli Spheroplast Membranes, Biophys. J. 107 (9) (2014) 2082–2090, https://doi.org/10.1016/j.bpj.2014.09.034.
[57] M.O. Onitsuka, Y. Rikihisa, H.B. Maruyama, Biochemical and topographical studies on Escherichia coli cell surface. IV. Giant spheroplast formation from a filamentous cell, J. Bacteriol. 138 (2) (1979) 567–574, https://doi.org/10.1128/jb.138.2.567-574.1979.
[58] Valap Sealant, Cold Spring Harb. Protoc. . 2015 (2015) pdb.rec082917. doi: 10.1101/pdb.rec082917.
[59] B. Miljevic, F. Hedayat, S. Stevanovic, K.E. Fairfull-Smith, S.E. Bottle, Z. D. Ristovski, To Sonicate or Not to Sonicate PM Filters: Reactive Oxygen Species Generation Upon Ultrasonic Irradiation, Aerosol Sci. Technol. 48 (12) (2014) 1276–1284, https://doi.org/10.1080/02786826.2014.981330.
[60] T.J. Mason, A.J. Cobley, J.E. Graves, D. Morgan, New evidence for the inverse dependence of mechanical and chemical effects on the frequency of ultrasound, Ultrason. Sonochem. 18 (1) (2011) 226–230, https://doi.org/10.1016/j.ultsonch.2010.05.008.
[61] J. Jordens, B. Bamps, B. Gielen, L. Braeken, T. Van Gerven, The effects of ultrasound on micromixing, Ultrason. Sonochem. 32 (2016) 68–78, https://doi.org/10.1016/j.ultsonch.2016.02.020.
[62] S. Nasseri, A.H. Mahvi, M. Seyedsalehi, K. Yaghmaeian, R. Nabizadeh, M. Alimohammadi, G.H. Safari, Degradation kinetics of tetracycline in aqueous solutions using peroxydisulfate activated by ultrasound irradiation: Effect of radical scavenger and water matrix, J. Mol. Liq. 241 (2017) 704–714, https://doi.org/10.1016/j.molliq.2017.05.137.
[63] N. Cerca, K.K. Jefferson, Effect of growth conditions on poly-N-acetylglucosamine expression and biofilm formation in Escherichia coli, FEMS Microbiol. Lett. 283 (2008) 36–41, https://doi.org/10.1111/j.1574-6968.2008.01142.x.
[64] N. Majdalani, S. Gottesman, The Rcs phosphorelay: A complex signal transduction system, Annu. Rev. Microbiol. 59 (1) (2005) 379–405, https://doi.org/10.1146/annurev.micro.59.050405.101230.
[65] K.E. Eboigbodin, C.A. Biggs, Characterization of the extracellular polymeric substances produced by Escherichia coli using infrared spectroscopic, proteomic, and aggregation studies, Biomacromolecules. 9 (2) (2008) 686–695, https://doi.org/10.1021/bm701043c.
[66] M. Vaara, Covalent structure of two novel neutrophile leucocyte-derived proteins of porcine and human origin, Microbiol. Rev. 56 (1992) 535–547, https://doi.org/10.1111/prd.12107.
[67] R.E.W. Hancock, Alterations in structure of the cell envelope, Ann. Rev. Microbiol. 38 (1984) 237–264.
[68] F.G. Ferris, T.J. Beveridge, Physiochemical roles of soluble metal cations in the outer membrane of Escherichia coli K-12, Can. J. Microbiol. 32 (1986) 594–601, https://doi.org/10.1139/m86-110.
[69] L. Leive, Release of lipopolysaccharide by EDTA treatment of E., coli, Biochem. Biophys. Res. Commun. 21 (4) (1965) 290–296, https://doi.org/10.1016/0006-291X(65)90191-9.
[70] H.-L. Alakomi, A. Paananen, M.-L. Suihko, I.M. Helander, M. Saarela, Weakening Effect of Cell Permeabilizers on Gram-Negative Bacteria Causing Biodeterioration, Appl. Environ. Microbiol. 72 (7) (2006) 4695–4703, https://doi.org/10.1128/AEM.00142-06.
[71] Q. He, D. Liu, M. Ashokkumar, X. Ye, T.Z. Jin, M. Guo, Antibacterial mechanism of ultrasound against Escherichia coli: Alterations in membrane microstructures and properties, Ultrason. Sonochem. 73 (2021) 105509, https://doi.org/10.1016/j.ultsonch.2021.105509.
[72] L. Zhang, H. Qi, Z. Yan, Y. Gu, W. Sun, A.A. Zewde, Sonophotocatalytic inactivation of E. coli using ZnO nanofluids and its mechanism, Ultrason. Sonochem. 34 (2017) 232–238, https://doi.org/10.1016/j.ultsonch.2016.05.045.
[73] M.A. de Pedro, F. Cava, Structural constraints and dynamics of bacterial cell wall architecture, Front. Microbiol. 6 (2015), https://doi.org/10.3389/fmicb.2015.00449.
[74] D.J. Waxman, J.L. Strominger, β-Lactam Antibiotics: Biochemical Modes of Action, ACADEMIC PRESS, INC. (1982), https://doi.org/10.1016/b978-0-12-506303-6.50009-1.
[75] L.D. Renner, D.B. Weibel, Cardiolipin microdomains localize to negatively curved regions of Escherichia coli membranes, Proc. Natl. Acad. Sci. U. S. A. 108 (15) (2011) 6264–6269, https://doi.org/10.1073/pnas.1015757108.
[76] K. Kikuchi, M. Sugiura, C. Nishizawa-Harada, T. Kimura, The application of the Escherichia coli giant spheroplast for drug screening with automated planar patch clamp system, Biotechnol. Reports. 7 (2015) 17–23, https://doi.org/10.1016/j.btre.2015.04.007.
[77] P. Jollès, J. Jollès, What's new in lysozyme research? - Always a model system, today as yesterday, Mol. Cell. Biochem. 63 (1984) 165–189, https://doi.org/10.1007/BF00285225.
[78] D.C. Birdsell, E.H. Cota-Robles, Production and ultrastructure of lysozyme and ethylenediaminetetraacetate-lysozyme spheroplasts of Escherichia coli, J. Bacteriol. 93 (1) (1967) 427–437, https://doi.org/10.1128/jb.93.1.427-437.1967.
[79] J.G. Voss, Lysozyme Lysis of Gram-Negative Bacteria without Production of Spheroplasts, J. Gen. Microbiol. 35 (2) (1964) 313–317, https://doi.org/10.1099/00221287-35-2-313.
[80] R.E. Wooley, J.L. Blue, In-vitro effect of EDTA-TRIS-lysozyme solutions on selected pathogenic bacteria, J. Med. Microbiol. 8 (1) (1975) 189–194.
[81] Ž. Pandur, I. Dogsa, M. Dular, D. Stopar, Liposome destruction by hydrodynamic cavitation in comparison to chemical, physical and mechanical treatments, Ultrason. Sonochem. 61 (2020) 104826, https://doi.org/10.1016/j.ultsonch.2019.104826.
[82] J. Zevnik, M. Dular, Liposome destruction by a collapsing cavitation microbubble: A numerical study, Ultrason. Sonochem. 78 (2021) 105706, https://doi.org/10.1016/j.ultsonch.2021.105706.
[83] T.C. Marentis, B. Kusler, G.G. Yaralioglu, S. Liu, E.O. Hæggström, B.T. Khuri-Yakub, Microfluidic sonicator for real-time disruption of eukaryotic cells and bacterial spores for DNA analysis, Ultrasound Med. Biol. 31 (9) (2005) 1265–1277, https://doi.org/10.1016/j.ultrasmedbio.2005.05.005.
[84] Ž. Pandur, D. Stopar, Evolution of mechanical stability from lipid layers to complex bacterial envelope structures (2020), https://doi.org/10.1016/bs.abl.2020.09.005.
[85] G. Van Den Bogaart, N. Hermans, V. Krasnikov, B. Poolman, Protein mobility and diffusive barriers in Escherichia coli : consequences of osmotic stress, Mol. Microbiol. 64 (2007) 858–871, https://doi.org/10.1111/j.1365-2958.2007.05705.x.
[86] W. Vollmer, P. Born, Bacterial cell envelope peptidoglycan, in: Microb. Glycobiol., Elsevier, 2010: pp. 15–28. doi:10.1016/B978-0-12-374546-0.00002-X.
[87] R.C. Hughes, P.F. Thurman, E. Stokes, Estimates of the porosity of Bacillus licheniformis and Bacillus subtilis cell walls, Z. Immunitatsforsch. Exp. Klin. Immunol. 149 (1975) 126–135. http://www.ncbi.nlm.nih.gov/pubmed/126549.
[88] B. Blasco, A.G. Pisabarro, M.A. de Pedro, Peptidoglycan biosynthesis in stationary-phase cells of Escherichia coli, J. Bacteriol. 170 (11) (1988) 5224–5228.
[89] M.A. Snowden, H.R. Perkins, Peptidoglycan cross-linking in Staphylococcus aureus. An apparent random polymerisation process, Eur. J. Biochem. 191 (2) (1990) 373–377, https://doi.org/10.1111/j.1432-1033.1990.tb19132.x.
[90] D. Gully, D. Gargani, K. Bonaldi, C. Grangeteau, C. Chaintreuil, J. Fardoux, P. Nguyen, R. Marchetti, N. Nouwen, A. Molinaro, P. Mergaert, E. Giraud, A Peptidoglycan-Remodeling Enzyme Is Critical for Bacteroid Differentiation in Bradyrhizobium spp. During Legume Symbiosis, Mol. Plant-Microbe Interact. 29 (6) (2016) 447–457, https://doi.org/10.1094/MPMI-03-16-0052-R.
[91] J. Frías, F. Ribas, F. Lucena, Substrate affinity from bacterial strains and distribution water biofilms, J. Appl. Bacteriol. 76 (1994) 182–189, https://doi.org/10.1111/j.1365-2672.1994.tb01614.x.